

Molecular beam epitaxial growth of Bi₂Se₃- and Tl₂Se-doped PbSe and PbEuSe on CaF₂/Si(111)

X. M. Fang,^{a)} I-Na Chao, B. N. Strecker, and P. J. McCann

School of Electrical and Computer Engineering and Laboratory for Electronic Properties of Materials, University of Oklahoma, Norman, Oklahoma 73019

S. Yuan

Department of Electronic Materials Engineering, Australian National University, Canberra, ACT 0200, Australia

W. K. Liu

Quantum Epitaxial Designs, Inc., Bethlehem, Pennsylvania 18015

M. B. Santos

Department of Physics and Astronomy and Laboratory for Electronic Properties of Materials, University of Oklahoma, Norman, Oklahoma 73019

(Received 1 December 1997; accepted 22 December 1997)

We report results on the incorporation of Bi (*n* type) and Tl (*p*-type) impurity in PbSe and PbEuSe grown on CaF₂/Si(111) by molecular beam epitaxy. Bi₂Se₃ and Tl₂Se were used as sources of dopants in the growth. Electron concentrations in the low 10¹⁹ cm⁻³ range and hole concentrations in the middle 10¹⁸ cm⁻³ range have been realized in the PbSe and PbEuSe layers with Eu content up to 3%. Electron and hole mobilities are comparable to those for PbSe and PbEuSe grown on BaF₂. © 1998 American Vacuum Society. [S0734-211X(98)09503-1]

I. INTRODUCTION

PbEuSe as an midinfrared material has recently been grown on PbSe substrates by molecular beam epitaxy (MBE).¹ The small lattice mismatch between PbEuSe and PbSe and the rapid increase in the bandgap of PbEuSe with increasing Eu content make PbEuSe/PbSe heterostructures useful for infrared devices. Diode lasers operating in the range of 3–8 μm have recently been fabricated in this material system.² High-quality epitaxial layers PbSe and PbEuSe can also be grown on (111)-oriented Si when fluoride buffer layers are used despite the large thermal expansion mismatch between PbSe, PbEuSe, and Si.^{3,4} Such heteroepitaxial growth offers a number of benefits that can lead to fabrication of improved infrared devices such as photovoltaic infrared sensor arrays.⁵

In most of recent work on the growth of lead salt on Si, both *n*- and *p*-type carrier concentrations were controlled by adjusting the crystal stoichiometry.³ Since the resulting vacancies have large diffusion coefficients, it is difficult to control *p*-*n* junction position with high precision.⁶ The vacancy concentrations, in the low 10¹⁸ cm⁻³ and 10¹⁷ cm⁻³ ranges for *n*- and *p*-type layers, respectively, are also relatively low for making light-emitting devices based on current injection. Recent work on the growth of PbSe and PbEuSe on PbSe substrates has used elemental Ag and Bi as *p*- and *n*-type dopants, respectively.^{1,2} Compared to Tl, another widely used *p*-type dopant in lead salt, Ag has a relatively large diffusion coefficient but it produces a less deep acceptor level for high-energy bandgap alloys thus reducing low-temperature freeze out of holes.⁷ Tl and Bi have been shown

to incorporate well in PbTe and PbSe under MBE growth conditions.^{1,8} In this work, we report results on the incorporation of Bi₂Se₃ and Tl₂Se in PbSe and PbEuSe grown on CaF₂/Si(111). Our results indicate that the use of Bi and Tl compounds helps maintain crystal stoichiometry. Electron concentrations in the low 10¹⁹ cm⁻³ range and hole concentrations in the middle 10¹⁸ cm⁻³ range have been realized in PbSe and PbEuSe with Eu content up to 3%. These carrier concentration levels that have been reached, are comparable to those used for making midinfrared diode lasers.² Despite the large thermal expansion mismatch between PbSe, PbEuSe, and Si, we show that the structural and electrical properties of the PbSe and PbEuSe layers grown on CaF₂/Si(111) are comparable to those for similar layers grown on BaF₂ substrates.

II. MBE GROWTH PROCEDURES

The growth of PbSe and PbEuSe on CaF₂/Si(111) was carried out in an Intevac Modular GEN II MBE system. Three-in-diam *p*⁺-type (0.005–0.025 Ω cm) and *n*⁺-type (0.001–0.004 Ω cm) Si wafers with offcut angles less than 0.3° were cleaned using a modified Shiraki method followed by dipping in a HF solution. By adding this dipping step, we have been able to reduce the Si thermal cleaning temperature by more than 300 °C so that unwanted reactions between Se and Si or Ca were avoided.⁹ Si wafers were outgassed in the buffer chamber at 200 °C for one hour before loaded into the growth chamber.

CaF₂ growth was accomplished by heating high-purity polycrystalline CaF₂ in a dual zone effusion cell held at 1280 °C. This cell temperature produces a beam equivalent pressure (BEP) for CaF₂ of 6.4×10⁻⁸ Torr and a growth

^{a)}Corresponding author; electronic mail: fang@phyast.nhn.ou.edu

rate of 0.007 ML/s calibrated from reflection high-energy electron diffraction (RHEED) intensity oscillation experiments.⁹ All CaF_2 layers were grown on thermally cleaned Si(111) at 700 °C. For Hall effect measurements, the thickness of CaF_2 layers was controlled in the range of 5–40 nm to provide good electrical isolation from the low resistivity substrate.

PbSe growth was accomplished by heating bulk PbSe in a low-temperature effusion cell. The effusion cell temperature was adjusted in the range of 635–710 °C to give a BEP of 1.3×10^{-6} Torr and a growth rate of 0.8 $\mu\text{m}/\text{h}$. For doping study, a 0.15 μm undoped PbSe buffer layer was grown on $\text{CaF}_2/\text{Si}(111)$ at 310 °C followed by growing a 2.2 μm Bi_2Se_3 -doped PbSe and a 0.15 μm undoped PbSe cap layer at 280 °C.

PbEuSe growth was accomplished by evaporating the bulk PbSe and elemental Eu from low-temperature effusion cells. Eu content is controlled by adjusting Eu flux rate. In this study, two Eu flux rates, 1% and 3% of that of PbSe, were used. To study the structural and electrical properties of PbEuSe, a 2.2 μm Bi_2Se_3 - or Tl_2Se -doped PbEuSe layer and a 0.15 μm undoped PbSe cap layer were grown on $\text{CaF}_2/\text{Si}(111)$ at 280 °C. Both Bi_2Se_3 and Tl_2Se were evaporated from fast dopant effusion cells with the BEPs in the range of 2.0×10^{-10} – 2.2×10^{-9} Torr and 5.0×10^{-11} – 2.3×10^{-10} Torr, respectively. An additional Se source was used to control the stoichiometry of the layers and keep the surface under Se rich condition. An (EPI) valved cracker was used to produce Se fluxes of 2.5% and 10% relative to PbSe flux for the growth of PbEuSe with 1% and 3% Eu, respectively.

The structural properties of the layers were characterized using a Philips high resolution x-ray diffraction (HRXRD) system with a four-crystal Ge(220) monochromator. The electrical properties of the samples were determined by Hall effect measurement at 77 and 300 K. Fourier transform infrared spectroscopy was used to investigate the shift of the PbEuSe absorption edge as a function of Eu content.

III. RESULTS AND DISCUSSION

At the initial stage, the growth of PbSe and PbEuSe on $\text{CaF}_2/\text{Si}(111)$ proceeds via a three-dimensional mode due to the high interfacial energy between the overlayer and the $\text{CaF}_2/\text{Si}(111)$ substrate. This is evidenced by the appearance of spots on RHEED patterns. However, the RHEED patterns gradually become streaky as the growth continues, indicating that a smooth surface starts to recover. The structural quality of the layers was confirmed by the occurrence of a weak (3×3) surface reconstruction in the $[\bar{1}10]$ and $[\bar{1}01]$ azimuths and sharp Kikuchi lines during the growth.

The surface of the layers looks mirror smooth. The cross hatches running along the three $\langle 110 \rangle$ directions are visible under a Nomarski optical microscope, indicating the thermal mismatch strain relief on cool down from the growth to room temperature.¹⁰

The tilts between PbSe, PbEuSe, and the crystallographic planes of Si(111) substrate as well as the full width at half

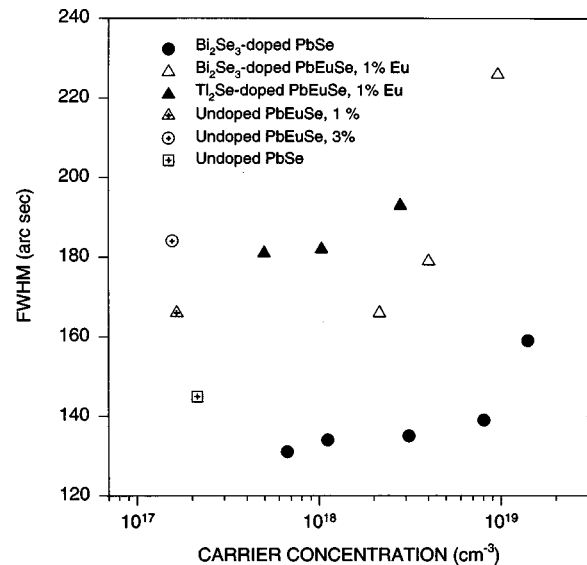


FIG. 1. Variation of the full width at half maximum of the Bragg (333) reflection for the Bi_2Se_3 -doped PbSe, Bi_2Se_3 - and Tl_2Se -doped PbEuSe layers grown on $\text{CaF}_2/\text{Si}(111)$.

maximum (FWHM) of the Bragg (333) reflection for the layers have been measured by HRXRD. The layer and Si substrate exhibit distinct periodic modulations of diffraction peak positions when the sample was rotated around its surface normal even though the offcut angle of the wafer is in the range of 0.1°–0.2°. The HRXRD data shows that the offcut direction of the substrate and the tilt direction of the layer are parallel to each other in consistence with Nagai's model¹¹ in which the tilt is a consequence of the surface steps and of the lattice mismatch. However, within the experimental uncertainty the tilts in all samples under investigation are some 40 arcsec and insensitive to the change in the offcut angle.

Figure 1 shows the FWHM of x-ray rocking curve for the Bi_2Se_3 -doped PbSe, Bi_2Se_3 - and Tl_2Se -doped PbEuSe layers grown on $\text{CaF}_2/\text{Si}(111)$ as a function of the room-temperature carrier concentration. It is seen from Fig. 1 that at relatively low concentrations, the FWHM for the PbSe layers increases slowly with increasing concentration. A significant increase in the FWHM occurs when the concentration exceeds $1 \times 10^{19} \text{ cm}^{-3}$. After incorporated with 1% and 3% Eu, the layers show dramatic increases in the FWHM. This is caused by the alloying effect associated with the Eu incorporation which may deteriorate the crystal quality. Interestingly, the FWHM for the PbEuSe layers doped with Tl_2Se is much wider than those doped with Bi_2Se_3 though all the samples were grown under the same conditions except using different dopant sources. This is probably caused by using Bi and Tl compounds rather than elements as sources of dopants. Compared to Tl_2Se , a Bi_2Se_3 molecule contains more Se atoms which could help maintain the crystal stoichiometry.⁷ Although a separate Se source was used in the growth, it is possible that there was insufficient Se for the Tl_2Se fluxes even though the Se flux is two orders of magnitude higher than the Tl_2Se ones. Our preliminary results

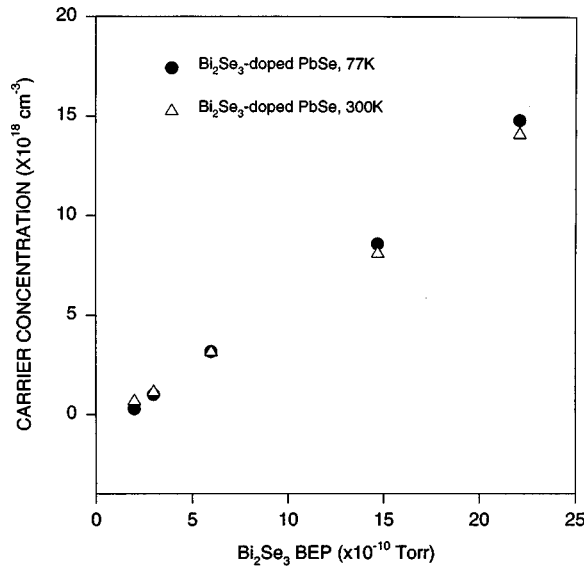


FIG. 2. Variation of the electron concentration in the Bi_2Se_3 -doped PbSe layers as a function of the beam equivalent pressure of Bi_2Se_3 .

show that Se deposited on a PbSe surface is rapidly desorbed at temperatures above 140–160 °C which is much lower than those for the growth of PbSe and PbEuSe. The effect of Se in adjusting the stoichiometry is also clearly seen from Fig. 1 by comparing the FWHM of the undoped PbSe with that of the Bi_2Se_3 -doped PbSe. No additional Se flux was applied in both cases. The Bi_2Se_3 -doped PbSe shows improved crystalline quality at low and moderate concentrations as compared with the undoped PbSe. That is probably because the Se

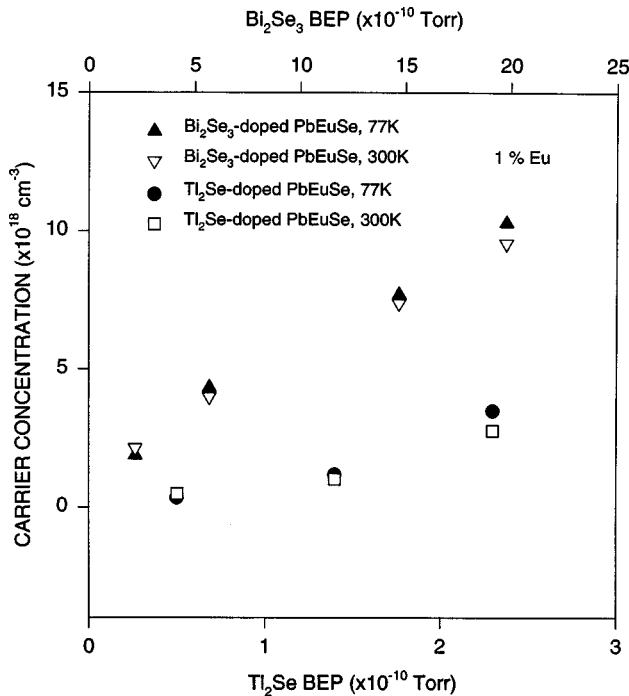


FIG. 3. Variation of the carrier concentrations in the Bi_2Se_3 - and Tl_2Se -doped PbEuSe layers with 1% Eu as a function of the beam equivalent pressures of Bi_2Se_3 and Tl_2Se .

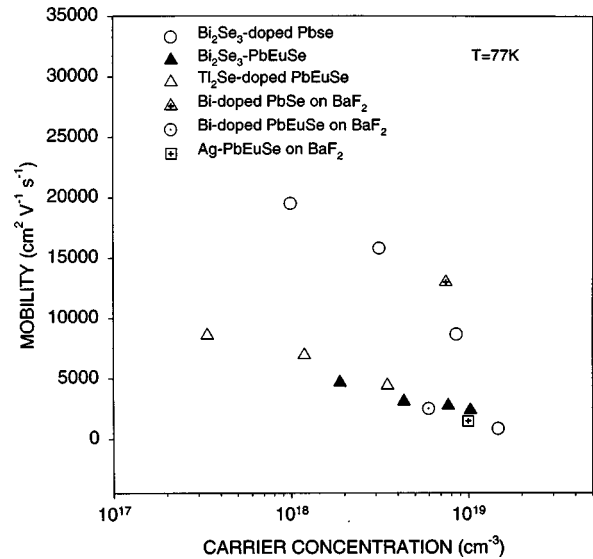


FIG. 4. Variation of the mobility at 77 K as a function of the carrier concentration for the Bi_2Se_3 -doped PbSe, Bi_2Se_3 - and Tl_2Se -doped PbEuSe layers along with the mobility data for PbSe grown on BaF_2 (Ref. 1).

species needed for maintaining the stoichiometry is supplemented by dissociation of Bi_2Se_3 molecules as they arrive on the surface.

Figures 2 and 3 show the variation of the carrier concentrations in the Bi_2Se_3 -doped PbSe, Bi_2Se_3 - and Tl_2Se -doped PbEuSe layers as a function of the BEPs of Bi_2Se_3 and Tl_2Se sources. It is seen from Figs. 2 and 3 that both the room-temperature and 77 K carrier concentrations increase with increasing the BEPs, indicating that the incorporation of Bi and Tl in PbSe and PbEuSe in the BEP range studied is near unity. At high BEPs, i.e., $\sim 2.2 \times 10^{-9}$ and $\sim 2.3 \times 10^{-10}$ Torr for Bi_2Se_3 and Tl_2Se , respectively, no decline in the carrier concentrations was observed, implying that there was no discernible segregation of Bi_2Se_3 and Tl_2Se in the PbSe and PbEuSe layers. Partin *et al.*⁸ observed a drop in hole concentrations for PbTe at Tl concentrations $> 10^{20} \text{ cm}^{-3}$ which is much higher than the impurity concentrations reached in this work. As seen from Figs. 2 and 3, all the samples exhibit weak low-temperature carrier freeze out at low BEPs, implying that the Bi-donor level is below the conduction band edge while the Tl-acceptor level is above the valence band edge. At high BEPs, however, the low-temperature carrier concentrations become larger than those obtained at room temperature. This behavior has also been observed for PbSrS and is probably a consequence of tem-

TABLE I. Thermal expansion coefficients and lattice constants of Si, CaF_2 , BaF_2 , and PbSe at room temperature.

Material	Lattice constant (\AA)	Thermal expansion coefficient at 300 K ($10^{-6}/\text{K}$)
Si	5.431	2.6
CaF_2	5.46	19.1
BaF_2	6.20	19.8
PbSe	6.12	19.4

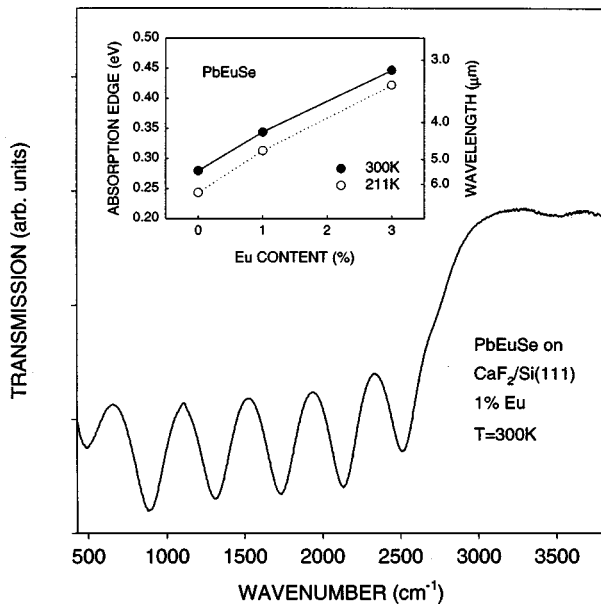


FIG. 5. Transmission spectrum of a PbEuSe layer with 1% Eu grown on $\text{CaF}_2/\text{Si}(111)$ obtained at 300 K. The inset shows the shift of the absorption edge of the PbEuSe layers as a function of the Eu content.

perature dependent degeneracy at high carrier concentrations as suggested by Holloway *et al.*¹² The Bi_2Se_3 - and Tl_2Se -doped PbSe and PbEuSe layers show electron and hole concentrations as high as 1.5×10^{19} and $3.5 \times 10^{18} \text{ cm}^{-3}$ at 77 K, respectively. These carrier concentration levels are nearly one order of magnitude higher than those achieved via vacancy doping and comparable to those used in making midinfrared diode lasers.²

Figure 4 shows the variation of the mobility at 77 K as a function of the carrier concentration for the Bi_2Se_3 -doped PbSe, Bi_2Se_3 - and Tl_2Se -doped PbEuSe layers grown on $\text{CaF}_2/\text{Si}(111)$ along with the mobility data for PbSe and PbEuSe grown on BaF_2 under similar conditions.¹ It is seen from Fig. 4 that the mobilities are as high as those for PbSe and PbEuSe layers grown on BaF_2 substrates. The low-temperature mobilities also show similar carrier concentration dependence as those for bulk PbSe.¹³ As seen from Table I, the thermal expansion and lattice mismatch between PbSe and Si are much larger than those between PbSe and BaF_2 . However, it has been shown that lead salt layers grown (111)-oriented Si with an intermediate fluoride buffer layer can relieve the thermal and lattice mismatch strain by misfit dislocations which glide on the primary (100) slip planes inclined with respect to the (111) surface.¹⁰ The results shown in Fig. 4 indicate that high-quality layers of

PbSe and PbEuSe can be grown on $\text{CaF}_2/\text{Si}(111)$ by MBE and exhibit electrical properties similar to those for PbSe grown on BaF_2 .

Figure 5 shows a room temperature transmission spectrum below and above the bandgap of a PbEuSe layer with 1% Eu grown on $\text{CaF}_2/\text{Si}(111)$ in the range of $400\text{--}3800 \text{ cm}^{-1}$ at normal incidence. Below 2800 cm^{-1} , the well-pronounced Fabry–Perot interference with periods of up to five dominate the spectrum. The inset of Fig. 5 shows the variation of the absorption edge of PbEuSe layers as a function of Eu content at temperatures of 211 and 297 K, respectively. For 1% Eu, the absorption edge shifts at a rate of 550 cm^{-1} per % Eu, while for 3% at a rate of 450 cm^{-1} per % Eu. It is seen from Fig. 5 that the absorption edge of the PbEuSe layer with 3% is shifted to $\sim 3.3 \mu\text{m}$.

IV. CONCLUSION

We have successfully grown Bi_2Se_3 - and Tl_2Se -doped PbSe and PbEuSe on $\text{CaF}_2/\text{Si}(111)$. The use of Bi and Tl compounds helps maintain the crystal stoichiometry. We have reached electron and hole concentrations that are nearly one order of magnitude higher than those obtained by vacancy doping. The electrical properties of the layers are comparable to those for PbSe grown on BaF_2 . The absorption edge of PbEuSe has been significantly shifted to $\sim 3.3 \mu\text{m}$ with only 3% Eu.

ACKNOWLEDGMENT

This work is supported by the National Science Foundation through Grant No. OSR-9550478.

- ¹P. Norton and M. Tacke, *J. Cryst. Growth* **81**, 405 (1987).
- ²M. Tacke, Beate Spanger, A. Lambrecht, P. R. Norton, and H. Böttner, *Appl. Phys. Lett.* **53**, 2260 (1988).
- ³H. Zogg, A. Fach, C. Maissen, J. Masek, and S. Blunier, *Opt. Eng. (Bellingham)* **33**, 1440 (1994).
- ⁴V. Mathet, P. Galtier, F. Nguyen-Van-Dau, G. Padeletti, and J. Olivier, *J. Cryst. Growth* **132**, 241 (1993).
- ⁵A. Fach, C. Maissen, J. Masek, S. Teodoropol, and H. Zogg, *Mater. Res. Soc. Symp. Proc.* **229**, 279 (1994).
- ⁶J. N. Walpole and R. L. Guldi, *J. Nonmetals* **1**, 227 (1973).
- ⁷D. L. Partin, *Semicond. Semimet.* **33**, 311 (1991).
- ⁸D. L. Partin, C. M. Thrush, S. J. Simko, and S. W. Gaarenstroom, *J. Appl. Phys.* **66**, 6115 (1989).
- ⁹P. J. McCann, X. M. Fang, W. K. Liu, B. N. Strecker, and M. B. Santos, *J. Cryst. Growth* **175/176**, 1057 (1997).
- ¹⁰H. Zogg, S. Blunier, A. Fach, C. Maissen, P. Müller, S. Teodoropol, V. Meyer, G. Kostorz, A. Dommann, and T. Richmond, *Phys. Rev. B* **50**, 10 801 (1994).
- ¹¹H. Nagai, *J. Appl. Phys.* **45**, 3789 (1974).
- ¹²H. Holloway and G. Jesion, *Phys. Rev. B* **26**, 5617 (1982).
- ¹³D. K. Hohnke and S. W. Kaiser, *J. Appl. Phys.* **45**, 892 (1974).